



# Thirteen years of air pollution hourly monitoring in a large city: Potential sources, trends, cycles and effects of car-free days

Mauro Masiol <sup>a,b,\*</sup>, Claudio Agostinelli <sup>b</sup>, Gianni Formenton <sup>c</sup>, Enzo Tarabotti <sup>d</sup>, Bruno Pavoni <sup>b</sup>

<sup>a</sup> Division of Environmental Health and Risk Management, School of Geography, Earth & Environmental Sciences, University of Birmingham, Edgbaston, Birmingham B15 2TT, United Kingdom

<sup>b</sup> Dipartimento di Scienze Ambientali, Informatica e Statistica, Università Ca' Foscari Venezia, Dorsoduro 2137, 30123 Venice, Italy

<sup>c</sup> Dipartimento Regionale Laboratori-Sede Operativa di Padova, Agenzia Regionale per la Prevenzione e Protezione Ambientale del Veneto, Via Ospedale Civile 22, 35121 Padova, Italy

<sup>d</sup> Dipartimento Provinciale di Venezia, Agenzia Regionale per la Prevenzione e Protezione Ambientale del Veneto, Via Lissa 6, 30174 Mestre, Italy

## HIGHLIGHTS

- 13 air pollutants were hourly measured for 13 years in a large city of NE Italy.
- Long-term, seasonal, weekly and daily patterns were investigated.
- Relationships with potential sources and photochemical processes are discussed.
- The effects on air quality of mitigation measures so far applied are evaluated.
- Results may help policy-makers to adopt more successful mitigation strategies.

## ARTICLE INFO

### Article history:

Received 29 April 2014

Received in revised form 25 June 2014

Accepted 28 June 2014

Available online 16 July 2014

Editor: P. Kassomenos

### Keywords:

Air quality  
Urban pollution  
Nitrogen oxides  
Ozone  
BTEX  
PM<sub>10</sub>

## ABSTRACT

Thirteen air pollutant concentrations were measured hourly for 13 years (2000–2013) at an urban background site of a large city in the eastern Po Valley (Italy) and results were chemometrically analysed. The pollutant list includes CO, NO, NO<sub>2</sub>, NO<sub>x</sub>, O<sub>3</sub>, SO<sub>2</sub>, benzene, toluene, ethylbenzene, *o*-, *m*- and *p*-xylenes and PM<sub>10</sub>, all known or suspected of having adverse effects on human health. The hourly data were statistically processed to detect the long-term trends in relation to the changes in the emission scenarios occurred in the last decade. The most probable emission sources and atmospheric photochemical processes were investigated by analyzing the seasonal, weekly, diurnal cycles of pollutants and the lagged correlations amongst pollutants. The role of micro-meteorological factors upon the air quality was assessed by analyzing the relationships with key weather parameters, while the location of the potential sources was studied by matching atmospheric circulation and pollution data through bivariate polar plots and conditional probability functions. In addition, a new statistical procedure is presented and tested to analyze the periods when common mitigation measures were adopted in the city (e.g., the total stop of traffic and car-free days) and to evaluate their real effect upon the air quality. By providing direct information on the levels and trends of key pollutants, this study finally enables some general considerations about air pollution in an important hotspot of Southern Europe, the eastern Po Valley, where the levels of some key pollutants are still far from meeting the EC limit and target values. It may help policy-makers to take successful mitigation measures.

© 2014 Elsevier B.V. All rights reserved.

## 1. Introduction

The worsening of air quality in highly anthropized environments exerts a high level of interest within the scientific community and public opinion because of the known strong relationship between exposure

to many air pollutants and increased adverse short- and long-term effects on human health (e.g., Maynard, 2009; Laumbach and Kipen, 2012). In addition, air pollution seriously impairs visibility (Hyslop, 2009), may damage materials in important buildings of the cultural heritage (Watt et al., 2009) and directly and indirectly affects the climate (Seinfeld and Pandis, 2006). Recently air pollution was also included as a IARC known carcinogen to human beings (group 1). In Europe, despite the EC legislative effort has driven an overall improvement of the air quality in the last two decades (Fenger, 2009), some hot-spots still remain. It is therefore imperative to focus the research on determining

\* Corresponding author at: Division of Environmental Health and Risk Management, School of Geography, Earth & Environmental Sciences, University of Birmingham, Edgbaston, Birmingham B15 2TT, United Kingdom.

E-mail address: [m.masiol@bham.ac.uk](mailto:m.masiol@bham.ac.uk) (M. Masiol).

the ambient levels of hazardous pollutants in the areas, where the limits proposed by international organizations (WHO, 2000) or imposed by the European Directives are not or not yet met, and a strong potential adverse effect on public health exists. This is the case of the Po Valley (Northern Italy).

This study analyzes a dataset of 13 airborne pollutants recorded at an urban background site in Mestre-Venice, a large city of the Po Valley, for 13-years (November 2000–November 2013): carbon monoxide (CO), nitrogen oxides ( $\text{NO}_x = \text{NO} + \text{NO}_2$ ), ozone ( $\text{O}_3$ ), sulphur dioxide ( $\text{SO}_2$ ), benzene, toluene, ethylbenzene, and *ortho*-, *meta*-, and *para*-xylenes (collectively known as BTEX) and particulate matter with an aerodynamic diameter of  $\leq 10 \mu\text{m}$  ( $\text{PM}_{10}$ ). CO is mainly generated by photochemical breakdowns of methane and nonmethane hydrocarbons as well as directly emitted by most anthropogenic combustion processes and its major sink is the oxidation by hydroxyl radical (Seinfeld and Pandis, 2006). Ozone is a reactive oxidant gas playing a key role in the photochemical air pollution and atmospheric oxidation processes. Although in the upper atmosphere it acts as a barrier for ultraviolet rays, in the troposphere it is a secondary air pollutant generated through a series of complex photochemical reactions involving solar radiation and ozone-precursors, i.e.  $\text{NO}_2$  and reactive hydrocarbons of biogenic (Curci et al., 2009) and anthropogenic (Hoor et al., 2009) origin.

Nitrogen oxides in urban environments are principally emitted from fossil fuel combustion as NO, which plays important roles in the atmospheric chemistry by rapidly reacting with ozone or radicals and forming  $\text{NO}_2$ . In the presence of sunlight,  $\text{NO}_2$  is then photolyzed by a short-wave solar radiation ( $\lambda < 398 \text{ nm}$ ) to NO and free oxygen. Such equilibrium, named photostationary state, describes the complex photochemistry of the  $\text{NO}$ – $\text{NO}_2$ – $\text{O}_3$  system in the lower troposphere, which, at a local scale, is dominated by a limited number of fast reactions including CO and many volatile organic compounds (VOCs). Because of the strong inter-conversion between ozone and  $\text{NO}_2$ , the level of oxidants ( $\text{OX} = \text{O}_3 + \text{NO}_2$ ) may give some insights into the oxidative potential of the atmosphere (Kley et al., 1999). Furthermore, increasing atmospheric  $\text{NO}_x$  concentrations may favour nitric acid formation as a result of the daytime gas phase recombination reaction of  $\cdot\text{OH}$  with  $\text{NO}_2$ , and have therefore a key role for the secondary inorganic aerosol generation (Finlayson-Pitts and Pitts, 2000).

Sulphur dioxide is emitted in the atmosphere from both natural (volcanoes, grassland, forest fires) and many anthropogenic sources involving the use of fossil fuels (crude oil and coal transformation processes, fossil fuel combustion, metal smelting and other industrial processes).  $\text{SO}_2$  may oxidize to  $\text{S(VI)}$  species and in this form it acts as a sulphate precursor in the aerosol system by modifying the direct and indirect radiative forcing and enhancing the acid deposition.

In urban environments BTEX are principally emitted by vehicular exhaust gases because of their presence in fuels and lubricating and heating oil. Other sources are gasoline evaporation, use of solvents and paintings, biomass burning, leakage from natural gas and liquefied petroleum gas. BTEX are highly reactive in the troposphere playing a key role in the atmospheric chemistry as important photochemical precursors for tropospheric ozone and secondary organic aerosol generation (Atkinson and Arey, 2003).

The main goals of this study are to: (1) detect the long-term trends in relation to the changes in the emission scenarios occurring in the last decade, including the technological improvements, the decline of many industrial activities and the construction of a new highway outside the city; (2) investigate the seasonal, weekly and daily cycles of pollutants to depict the most probable emission sources and photochemical processes; (3) study the inter-species relationships and their lagged correlations with some weather parameters to detect the role of micro-meteorological factors upon the air quality and (4) assess the location of the potential sources by combining atmospheric circulation and pollution data through bivariate polar plots and conditional probability functions. In addition, a new statistical procedure is presented and

tested to investigate the periods when extreme mitigation measures, such as the total stop of traffic and car-free days, were adopted in the city. Results are then discussed to assess the real effects upon the air quality and to help policy-makers to adopt successful mitigation strategies. A summary of the potential harmful effects upon human health is presented in Supplementary Information Table SI1.

## 2. Materials and methods

### 2.1. Study area: emission sources and weather

Mestre (Fig. 1) is a large mainland city where most of the population of Venice Municipality live: 271,000 inhabitants in 2001 and 263,000 in 2011 (ISTAT, 2012). It is located in the eastern part of the Po Valley, between the Adriatic Sea and a heavily anthropized mainland, 9 km WNW from the historic city centre of Venice, which lies in the middle of a  $\sim 550 \text{ km}^2$  wide coastal lagoon. The main anthropogenic emissions include:

- the southern conurbation of Mestre includes Porto Marghera, one of the widest industrial areas of Italy, with many chemical and metallurgical works, oil-refineries and storage, building material, ceramics, shipbuilding and glass industries, incineration and thermoelectric power plants burning coal and refuse-derived fuel, wastewater treatment, hazardous waste incineration and other factories. Its development reached a maximum of 33,000 employees in the late '60s, followed by a rapid decline in industry: in 2011 the number of industries was 690 and the number of employees was  $\sim 11,000$  (EZI, 2012);
- frequently traffic congested roads, mainly during peak hours (7–9 am, 6–8 pm). A very busy ring road passes within Mestre and acts as a junction between two main highways (European route E70) with more than 75,000 vehicles per day,  $\sim 14\%$  heavy duty vehicles (CAV, 2011). Since 2009, most of this traffic was diverted outside of Mestre through the new A57 highway. Route E55 connecting the Central to the Southern Europe also passes through the study area. From 2004 to today, the closure of a number of main roads for the construction of the tram network has further jammed the traffic in the city;
- domestic heating, which burns predominantly methane in urban areas; however the use of wood/pellet stoves is becoming a widely used alternative in Northern Italy;
- an international airport about 9 km NE of Mestre, the third in Italy for flying traffic, counting more than 4 million passengers per year in 2001 and about twice in 2011 (SAVE, 2012);
- an industrial harbour and a main cruise ship terminal. In 2009, the total trade of the port of Venice counted about 25 million tons and 1,887,276 passengers, for the passage of approximately 4300 individual ships (Venice Port Authority, 2010).

The high levels and the frequent exceedings of the European limit and target values in the study area for many air pollutants are inevitably due to this complex emissive scenario, but they are also significantly favoured by orographic factors limiting the dispersion of pollutants. The worst air quality is observed during the coldest season due to frequent and prolonged wind calm periods, atmospheric stability, persistent thermal inversions and lower planetary boundary layer heights during the night-time. In addition, since the study area is located in a coastal zone bordered by the Po Valley, the influence of the atmospheric circulation and long-range transports from the mainland can play important roles in the accumulation and removal of locally emitted air pollutants. Fig. 1 shows the wind roses on seasonal basis: annually dominant winds blow from NNE and W and NE winds increase during the cold season. Direction from SE is however predominant in the warmest months due to sea breezes, which bring air masses from the Adriatic Sea to the mainland during the daytime.

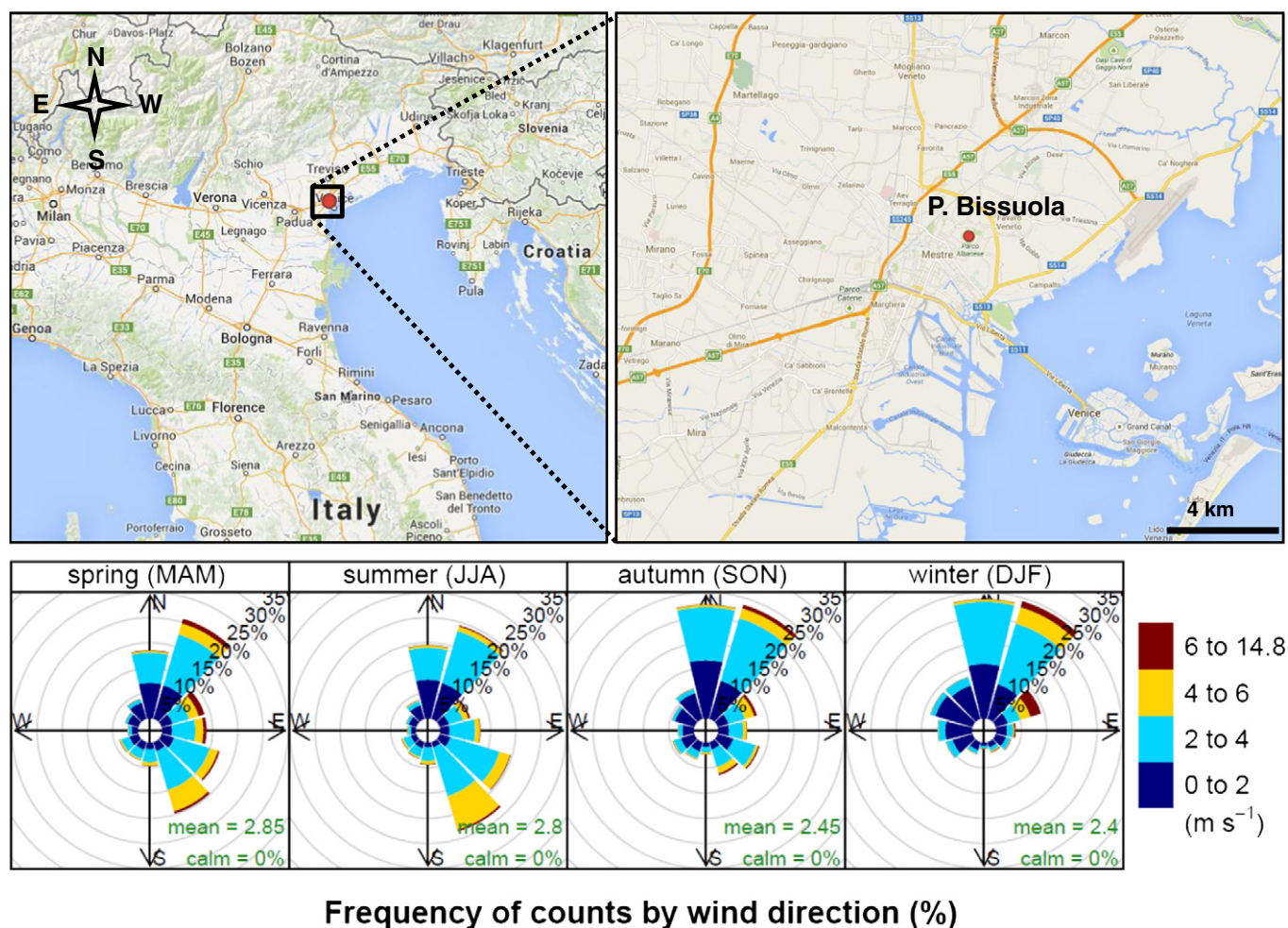


Fig. 1. Map of the NE Italy (up left), location of the sampling site in Mestre-Venice (up right) and wind roses on seasonal basis (bottom).

## 2.2. Experimental

The sampling site (Lat.  $45^{\circ}29'58.42''$  N; Long.  $12^{\circ}15'40.50''$  E) is located in an  $\sim 0.4 \text{ km}^2$ -wide public park within the main residential area of Mestre (Fig. 1) and is operated by the local environmental protection agency (ARPAV). Data are hourly measured with automatic instruments following the European standards: EN 14626:2012 for CO, EN 14211:2012 for NO, NO<sub>2</sub>, and NO<sub>x</sub>, EN 14212:2012 for SO<sub>2</sub>, EN 14625:2012 for O<sub>3</sub>, and EN 14662-3:2005 for benzene. Methods compatible with the in-use European standards were adopted in the period preceding their promulgation. PM<sub>10</sub> measurements started in June 2009 and used beta gauge monitors with a 2 h time resolution. Quality assurance and quality control procedures followed the national and ARPAV standards (ARPAV, 2014): CO, NO<sub>x</sub>, O<sub>3</sub> and SO<sub>2</sub> instruments are calibrated daily and those for BTEX once a month. Validation experiments are conducted for PM<sub>10</sub> between gravimetric and automatic procedures; several tests are also performed routinely (at least 1 test every week) to keep a constant check on the automatic samplers. Pairs of filters are measured with both methods and the results are checked to ensure that they are within the variation margins imposed by the technical protocols adopted in UNI EN 12341:2001. From January 2006, 24-h samplings of PM<sub>10</sub> were carried out according to the EN 12341:1998 standard and masses were gravimetrically measured. Devices are fully serviced. Ambient temperature, wind speed (WS) and direction data, relative humidity (RH) and atmospheric pressure were hourly recorded at a nearby weather station.

## 2.3. Data handling and statistical procedures

A preliminary evaluation and data clean-up were performed to create a significant and robust dataset. Since the main objective of the study is to depict general trends, the presence of outliers linked to casual and single episodes was checked: (i) BTEX data in 4 days (few hours every day) were eliminated because of the presence of extremely high outliers, mostly due to graffiti spray vandalisms in the surroundings of the site; and (ii) all data above the 99th percentile were not included in the computations.

All statistical elaborations were performed using R (R Core Team, 2013). A seasonal-trend decomposition procedure of time series based on 'Loess' (STL) was applied to investigate the long-term and seasonal variations of pollutants recorded over at least 10 consecutive years. Details of STL are reported in Cleveland et al. (1990), while some case studies using this technique can be found in Bigi and Harrison (2010) and Bigi et al. (2012). Since STL is calculated over monthly time series, which generally do not have normal distributions, the monthly median concentrations were used as input data and STL was performed in a robust mode.

Since the levels of many air pollutants can be related to both local and external sources, an investigation on the location of the sources was conducted. Bivariate polar plots and conditional probability function (CPF) plots were computed using R package 'openair' (Carslaw and Ropkins, 2012; Carslaw, 2013) to link pollutant levels to the local atmospheric circulation and detect the most probable local sources. A



detailed explanation of these methods is reported elsewhere (Ashbaugh et al., 1985; Carslaw et al., 2006). Briefly, polar plots map the pollutant concentrations by wind speed and direction as a continuous surface; surfaces are calculated through modelling by using smoothing techniques (Carslaw, 2013); CPFs show which wind directions are characterized by high concentrations (>90th percentile, in this case) and returns the probability of the occurrences.

The most common measure adopted for the mitigation of air pollution in major cities of Northern Italy is the partial suspension of urban traffic: the number of circulating vehicles within urban areas is limited on the basis of even or odd numbers of licence plates or/and EURO 0, I and II vehicles are stopped. In the case of very high pollution events, the total ban of traffic on Sundays is taken as an extreme measure. Furthermore, similar to other cities worldwide, some car-free days, so-called 'ecological Sundays', are adopted to encourage motorists to give up cars for a day. During these days, collectively named traffic restricted Sundays (TRS), the traffic in the urban road within the city centre is almost absent. A method to analyze the real benefit of traffic stopping events upon the air quality is here presented and validated with the data. A comprehensive explanation is given as Table SI2. Since the day-to-day levels of monitored pollutants are largely affected by seasonality, long-term trends and various weather factors, resulting in overall large noisy variations, the adopted procedure aims to limit such effects and allow a comparison between the TRS and non-TRS days. Briefly: (1) for every TRS, its three days-long hourly series (Saturday to Monday,  $I_t$ ) is extracted and processed together with the same periods of the 3 weeks forward and 4 backward for all the years,  $I_{t \pm n}$ ; (2) the  $I_{t \pm n}$  series that are in turn TRS or having less than 90% of available hourly data are eliminated; (3) the  $I_t/I_{t \pm n}$  ratios are calculated and log-transformed to return values (log-ratios) oscillating around zero; (4) cubic spline functions are applied to the log-ratios to interpolate the series and impute missing values; and (5) the spline log-ratios are plotted and the 50th and 90th percentile confidence bands are then calculated using the modified half-region depth method (Lopez-Pintado and Romo, 2011). The log-ratio trends are thus investigated in relation to other  $I_{t \pm n}$  and confidence intervals.

### 3. Results and discussion

In urban environments the gaseous pollutants, analysed in this study, are mainly emitted by mobile and stationary combustion processes or/and are directly/indirectly involved in complex photochemical processes. While atmospheric processes are mainly driven by actinic fluxes and oxidant species (e.g., ozone, nitrogen dioxide, hydroxyl and other radicals), the anthropogenic emissions may vary as a consequence of changes in human processes and habits. Therefore, the long-term

variations and the seasonal, weekly and daily patterns are to be discussed in relation to both weather and anthropogenic factors.

Table 1 summarizes some statistics of data. The decreasing average concentrations (in  $\mu\text{g m}^{-3}$ ) over the whole sampling period followed the order: CO (486) > NO<sub>x</sub> (62) > O<sub>3</sub> (40) > PM<sub>10</sub> (36) > NO<sub>2</sub> (32) > NO (19) > toluene (5.1) > SO<sub>2</sub> (3) > *m*-xylene (2.2) > benzene (1.8) > ethylbenzene (1.3) > *o*-xylene (1.3) > *p*-xylene (1). The time series of monthly averaged concentrations are plotted in Fig. 2: all the airborne pollutants except SO<sub>2</sub> showed an evident seasonality. If the results averaged over 13 years are compared with the current annual EC limit and target values, no exceeding is evident. Generally, CO, SO<sub>2</sub> and benzene levels were relatively low in all the study period and their thresholds, target and limit values were never exceeded. The annual average NO<sub>2</sub> concentrations only exceeded the EC limit (40  $\mu\text{g m}^{-3}$ ) in 2003, while the NO<sub>x</sub> annual limit value for the protection of vegetation (30  $\mu\text{g m}^{-3}$ ) was always breached, except in 2005. On the contrary, ozone levels in the study area were critical, as for most of the urban sites in southern Europe (EEA, 2014), and alert thresholds and limit/objective values were frequently exceeded. For example, in 2012 the EC human health threshold value for ozone was exceeded in 2 days, but the long-term objective for the protection of human health was breached for a total of 60 times. By analyzing gravimetric data, PM<sub>10</sub> annual average concentrations were exceeded in 2006 and 2007 (47  $\mu\text{g m}^{-3}$ ), but were never breached during 2008–2012 (33 to 39  $\mu\text{g m}^{-3}$ ). However, although in recent years the annual limit was met, the 50  $\mu\text{g m}^{-3}$  daily limit not to be exceeded up to a maximum of 35 days over a calendar year was always breached in all the study period.

#### 3.1. Long-term variations

The study period includes some relevant changes in the emissive scenario of Mestre-Venice, such as the decline of Porto Marghera industries, the transition from gasoline with tetraethyl lead as an anti-knock additive to unleaded petrol and the use of catalytic converters following the technological improvements EURO III (2000), EURO IV (2005) and EURO V (2009). Fig. 3a shows the long-term trends (solid line) and the 95th percentile confidence levels (dotted lines) computed by bootstrapping the data ( $R = 5000$ ,  $\alpha = 0.05$ ). STL for CO was limited to April 2002–March 2012 because of the lack of data. PM<sub>10</sub> was computed using daily collected data both gravimetrically (2006–2011) and with beta gauge (2012–2013): the two methods were carefully validated and data were consistent. Results show general decreases for CO, SO<sub>2</sub>, BTEX and PM<sub>10</sub>, while nitrogen oxides are almost steady (considering the confidence ranges) and ozone is slightly increasing. While the decline in the levels of CO was almost constant in the period, SO<sub>2</sub> exhibited a substantial drop in the 2000–2005 and BTEX decreased in two

**Table 1**

Statistics of measured data. N obs. = number of total observations. a) CO was measured until April 2012 and b) PM<sub>10</sub> was measured from June 2009 to November 2012.

	CO <sup>a</sup> mg m <sup>-3</sup>	NO μg m <sup>-3</sup>	NO <sub>2</sub> μg m <sup>-3</sup>	NO <sub>x</sub> μg m <sup>-3</sup>	O <sub>3</sub> μg m <sup>-3</sup>	SO <sub>2</sub> μg m <sup>-3</sup>	Benzene μg m <sup>-3</sup>	Toluene μg m <sup>-3</sup>	Ethylbenzene μg m <sup>-3</sup>
N obs.	88,314	103,813	103,677	103,826	104,888	104,797	102,074	101,020	102,202
Minimum	0	0	0	0	0	0	0	0	0
Median	0.3	3	29	36	30	2	1.1	3.1	1
Mean	0.5	19	32	62	40	3	1.8	5.1	1.3
Maximum	2.2	216	96	398	151	27	10.2	35	7.4
	<i>o</i> -xylene μg m <sup>-3</sup>	<i>m</i> -xylene μg m <sup>-3</sup>	<i>p</i> -xylene μg m <sup>-3</sup>	PM <sub>10</sub> <sup>b</sup> μg m <sup>-3</sup>	NO/NO <sub>2</sub> –	NO <sub>2</sub> /NO <sub>x</sub> –	Benzene/toluene –	OX –	Ambient temperature (°C)
N obs.	102,254	101,759	102,198	30,007	103,592	104,639	100,456	97,823	111,847
Minimum	0	0	0	0	0	0	0	1	–8.1
Median	0.9	1.3	0.6	28	0.17	0.81	0.36	69	14.7
Mean	1.3	2.2	1.0	36	0.45	0.72	0.43	74	14.9
Maximum	8.2	15.9	6.8	160	4.31	1.00	1.63	177	38.4

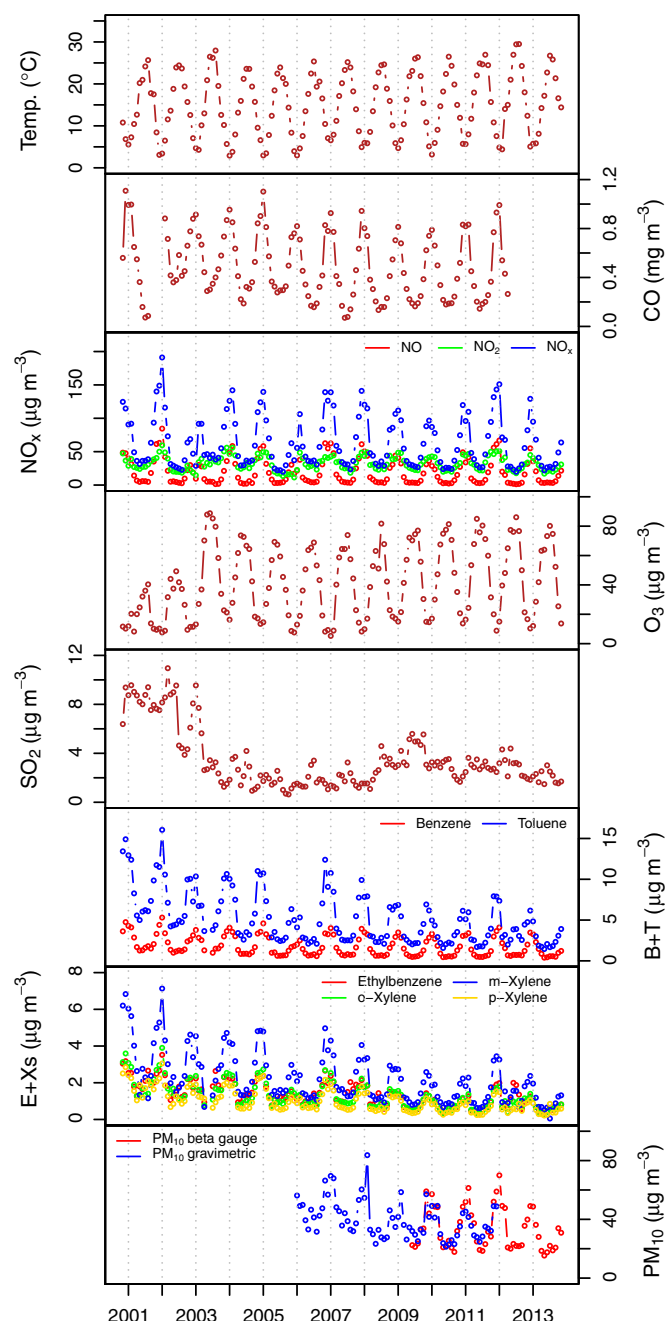


Fig. 2. Time series of monthly-averaged concentrations of measured air pollutants.

**Table 2**  
Traffic restricted Sundays (TRS) imposed in the study area since November 2001.

Year	Total closure of traffic on Sundays	Ecological Sundays
2002	20 Jan	12 May, 16 Jun, 22 Sep
2003	–	9 Mar, 6 Apr, 11 May, 22 Sep
2004	15 Feb	–
2005	23 Jan, 20 Feb	–
2006	19 Feb, 5 Mar, 19 Mar (8 am–7 pm)	–
2007	–	28 Jan, 25 Feb, 25 Mar
2008	–	27 Jan, 24 Feb, 30 Mar
2009	–	25 Jan, 1 Mar, 29 Mar
2010	–	24 Jan, 28 Feb
2011	–	20 Feb, 20 Mar
2012	–	26 Feb, 15 Apr
2013	–	10 Mar, 14 Apr

main steps: between 2000 and 2003, and in 2008–2010. Long-term trend of  $PM_{10}$  consistently dropped from 2006 and 2011. The toluene to benzene (T/B) ratio was used as a diagnostic indicator for vehicular traffic and underwent a quite constant decrease from 3.5 in 2000 to 2 in 2012. Comparable results are reported in the literature (e.g., Vardoulakis et al., 2002; Khoder, 2007), suggesting the vehicular traffic as a main polluting source (Caselli et al., 2010). Different from other European cities, the  $NO_2/NO_x$  trend was almost constant over the period: no significant increase of  $NO_2$  with respect to  $NO$  has been recorded. The levels of oxidants (OX) showed a general increase from 2000 to 2013 and an anomalous peak in 2003, which was mainly due to the concurrent increases of both ozone and  $NO_2$ . It was reported (Solberg et al., 2008) that the European summer of 2003 was exceptionally hot with a subsequent growth of surface ozone levels all over the central Europe, showing the highest values since the end of the 1980s. The effect of this extreme summer has been recorded in the study area and the subsequent increase of  $NO_2$  was a probable consequence. It is interesting to note that  $NO_2$  annual average levels only breached the EC limit in 2003. The role of ozone when interpreting the past and future high levels of  $NO_2$  should be attentively considered.

In addition, the quantification of the trends was evaluated by computing the Theil–Sen nonparametric estimator of slope (Sen, 1968; Theil, 1992) on the de-seasonalized monthly means. Since missing data can significantly affect results, only months having more than 50% of available data were included in the computations. The results are listed as Table S13 along with the upper and lower 95th confidence intervals and the  $p$ -values, which indicate how statistically significant is the slope estimation. Results show that the annual change of concentrations followed the order (in  $\mu g\ m^{-3}\ yr^{-1}$ ):  $CO\ (-20) < PM_{10}\ (-1.42) < NO_x\ (-0.92) < toluene\ (-0.4) < NO_2\ (-0.39) < NO\ (-0.31) < m\text{-xylene}\ (-0.19) < SO_2\ (-0.15) < ethylbenzene\ (-0.12) < o\text{-xylene}\ (-0.11) < p\text{-xylene}\ (-0.09) < benzene\ (-0.08) < O_3\ (1.23)$ .

By comparing the STL results with the emission inventories (EIs) for the Province of Venice in 2000, 2005 and 2010 (ISPRA, 2014, Supplementary Material Fig. S11), a general good agreement is evident for  $CO$ ,  $SO_2$  and benzene:

- $CO$  emissions dropped from  $71 \cdot 10^3$  Mg in 2000 to  $40 \cdot 10^3$  Mg in 2010, which reasonably agrees with the experimental data, and the main sources in the 2000–2010 period were road transports (average 49%), residential biomass boilers (16%), marine traffic (15%) and aluminium industry (8%). However, the decrease of  $CO$  was substantially driven by the drop of road traffic emissions from 2000 ( $43 \cdot 10^3$  Mg) to 2010 ( $14 \cdot 10^3$  Mg) following the technological improvements of car fleet. This was evident, even though an increase of biomass burning emissions ( $6 \cdot 10^3$  to  $34 \cdot 10^3$  Mg) was recorded, due to the growing use of wood for domestic heating;
- $SO_2$  emissions dropped from  $26 \cdot 10^3$  Mg in 2000 to  $5 \cdot 10^3$  Mg in 2010 and were generally related to power plants (average 63%), oil refineries (15%), combustion in manufacturing industry (7%) and harbour activities (5%). The main emission changes were recorded for power plant emissions ( $17 \cdot 10^3$  Mg in 2000 to  $1.2 \cdot 10^3$  Mg in 2010);
- Benzene was mainly emitted by road transport (average 56%), national sea traffic (17%), processes in petroleum industries (9%) and solvent use (5%); the main drop of emissions followed the decrease in road transport ( $183$  Mg in 2000 to  $51$  Mg in 2010);

On the contrary, the decreases of  $NO_x$  emissions estimated by EIs have not been confirmed by experimental data analysis. In the study period, combustion in energy and transformation industries mostly accounted for  $NO_x$  emissions (average 34%, mainly from power plants), followed by road traffic (32%) and other mobile sources and machinery (20%, mostly from harbour activities). A general drop of  $NO_x$  was reported by EIs, mainly driven by decreasing emissions in power plants ( $11 \cdot 10^3$  Mg in 2005 to  $2 \cdot 10^3$  Mg in 2010) and road traffic ( $10 \cdot 10^3$  Mg in 2000 and  $8 \cdot 10^3$  Mg in 2010).

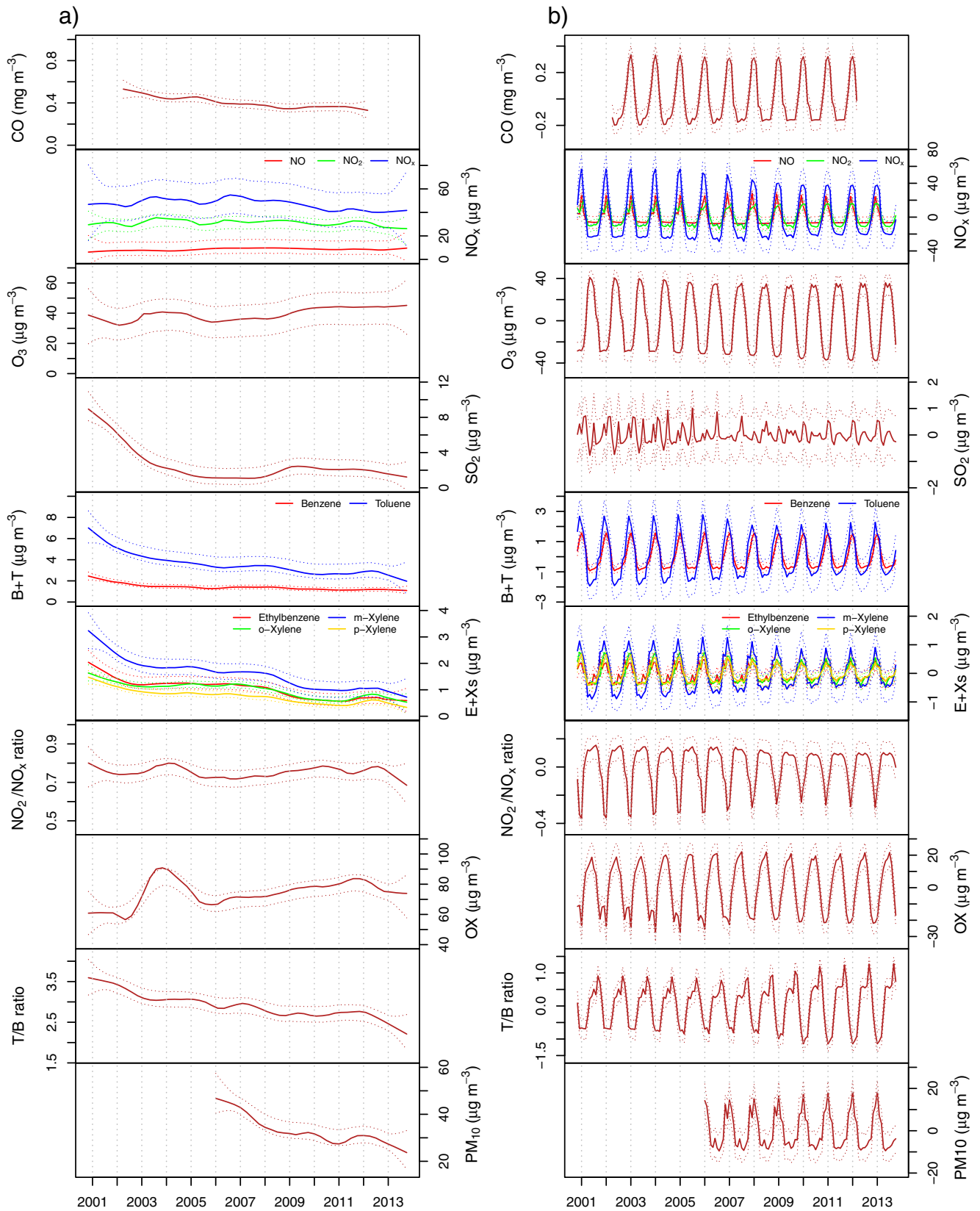


**Fig. 3.** Results of STL analysis: a) long-term trends (left) and b) de-trended seasonal components (right). Trends and seasonal patterns are in solid line, while the 95th percentile confidence levels computed by bootstrapping the data are in dotted lines.

In Europe, the recent discrepancy between the NO<sub>x</sub> emission reductions to be achieved and the NO<sub>2</sub> concentrations actually recorded, which do not meet the targets in many locations, raised the attention

of the scientific community toward NO<sub>x</sub> and NO–NO<sub>2</sub> partitioning (e.g., Grice et al., 2009; Cyrus et al., 2012). The increasing NO<sub>2</sub>/NO<sub>x</sub> ratio has been recently related to the growing proportion of diesel-



powered vehicles, which are known to have higher primary (direct) emissions of  $\text{NO}_2$ . However, experimental data reveal no significant trends in  $\text{NO}_2/\text{NO}_x$  ratios.

### 3.2. Seasonal patterns

The monthly-resolved distributions of air pollutants and weather parameters are reported as boxplots in Fig. SI2, while the seasonal patterns modelled by STL analysis are reported in Fig. 3b. All the pollutants exhibit evident seasonal cycles, except  $\text{SO}_2$ , which has no clear seasonality. The shaping of the cycles mainly derives from the interaction of emission factors, chemical processes occurring in the air and weather, which strongly affect the atmospheric dispersion conditions. Similar seasonal cycles were also reported in N Italy, for example in Modena, a large city in the southern-central Po Valley (Bigi et al., 2012). Being mainly generated through photochemical reactions, ozone presents the highest values during the warmest period (Apr–Sep), when the solar radiation is higher (Fig. SI2) and the atmosphere is more reactive. CO, NO,  $\text{NO}_2$ ,  $\text{NO}_x$ , all BTEX and  $\text{PM}_{10}$  show opposite seasonal cycles, with the highest values in the coldest months (January–December). Such patterns are mainly attributed to: (i) the raising of domestic emissions in the coldest months; (ii) the drop of ozone, the subsequent drop of hydroxyl radical and, thus, the limited oxidation potential in winter and (iii) the lower mixing layer heights in winter, the lower average wind speed and higher percentage of wind calm hours (Fig. SI2) commonly recorded in winter, which limit the dispersion capacity of the atmosphere. This seasonal pattern was commonly reported in the study area for other air pollutants, such as PM-bound nitrate (Squizzato et al., 2013) and PM-bound polycyclic aromatic hydrocarbons (Masiol et al., 2012a). Furthermore, it can be noted that the levels of winter peaks of CO,  $\text{NO}_x$  and BTEX extend for 1–2 months, while low concentrations in summer generally last longer (3–4 months), and secondary minor peaks of ethylbenzene and xylenes appear in October. This latter behaviour is unclear, but the switching on of the domestic heating, which commonly occurs in the region on October 15th, may play a role. STL decomposition further evidences the presence of decreasing amplitudes of the seasonal cycles for  $\text{NO}_x$  and BTEX. While for BTEX the decreasing amplitude can be explained by the drop of concentrations in long-term trends, this behaviour is unclear for nitrogen oxides, which have no evident long-term trends. The T/B ratio shifts from about 4 in the warmest season to 2 in winter and its seasonal pattern is at constantly increasing amplitudes.

The lack of seasonal patterns of  $\text{SO}_2$  is quite unexpected: while its main sources, as reported by EIs (power plant and harbour activities), generally rise during the warmest season due to the growing of both energy demand for air-conditioning and tourist cruise traffic, the highest levels of ozone and hydroxyl radical may enhance its fast oxidation to  $\text{SO}_3$  and the subsequent reaction with water vapour to sulphuric acid.

### 3.3. Daily and weekly cycles

Fig. SI3 reports the average daily patterns of the mean hourly concentrations calculated for the study period, while Fig. 4 shows the cycles for the cold and warm semesters. The semesters were set in correspondence of the daylight saving time start and end dates, which clearly shifts the anthropogenic emissions and roughly corresponds to the periods in which domestic heating is commonly switched off and on in the study area. Similar to seasonal patterns, daily cycles are the result of an interplay among emission strength, photochemical processes and micro-meteorological factors. Ozone has an evident daily peak corresponding to the mid-afternoon, i.e. the hours with higher solar irradiation, and its extent is the widest in the warm semester, following the sunlight time. Daily cycles of  $\text{SO}_2$  are similar to ozone, with higher levels in the central day and this pattern is enhanced in summer. Since the daylight hours of the warm season are characterized by the presence

of sea breezes, an influence of the local circulation pattern on the levels of  $\text{O}_3$  and  $\text{SO}_2$  should be considered.

Generally, CO, NO,  $\text{NO}_2$ ,  $\text{NO}_x$  and BTEX show typical patterns for urban areas: two daily peaks mainly corresponding to the hours of the heaviest vehicular traffic (7–9 am and 6–8 pm). The morning and evening modes are divided by a minimum, which is assumed to be the result of: (i) lower emissions (less traffic); (ii) larger availability of ozone driving the daylight photolysis of  $\text{NO}_x$  and the oxidation of CO and BTEX and (iii) enhanced atmospheric dispersion potential. This latter effect is more pronounced in summer, when ozone levels are higher and the local atmospheric circulation during daytime is dominated by the sea breezes, which have a key role in blowing air masses from the sea.

While the evening peak of CO and BTEX is dominant and extends longer than the morning one, mainly due to the drop of the mixing layer height and the enhanced night-time atmospheric stability, the two daily peaks of nitrogen oxides strongly differ between the cold and warm semesters. T/B ratio has a peculiar weekly and daily pattern, which is evident in warm seasons and is mostly due to the different reactivities in the atmosphere: toluene is 5 times as reactive as benzene in reacting with hydroxyl radicals (e.g., Baltaretu et al., 2009).

$\text{NO}$  generally presents a dominant morning peak and the evening peak is almost lacking in warm seasons and Sundays revealing its prevailing origin from road traffic.  $\text{NO}_2$  morning peak is dominant in summer but not in winter and the evening peak appears to be slightly shifted. It is assumed that the primary emissions of NO from vehicular traffic causing the morning peak will be quickly and almost completely oxidized in the warm season to  $\text{NO}_2$  due to higher  $\text{O}_3$  levels.

$\text{PM}_{10}$  presents two peculiar weekly cycles: two peaks of concentrations were generally recorded in correspondence of the peaks of traffic and are probably due to the resuspension of road dust materials. However, as for gaseous pollutants, particulate matter is also affected by the dispersion driven by the daily cycles of the mixing layer. Fig. 4 also evidences the weekday/weekend differences: CO, nitrogen oxides, and BTEX clearly show lower concentrations during weekends, while  $\text{SO}_2$  and  $\text{PM}_{10}$  show no evident differences. On the contrary,  $\text{O}_3$  increases during the weekends, further underlining its interplay with nitrogen oxides. The weekday/weekend variations of the daily cycles further show that the morning peaks of all traffic-related pollutants are less pronounced on Saturdays and almost absent on Sundays, while ozone peaks are higher. However, the total oxidant potential of the atmosphere (OX) appears to be fairly identical throughout the week, i.e. the lack of nitrogen oxides is compensated by the rising of ozone levels.

### 3.4. Relationships between pollutants and weather

Being chemical species emitted by similar anthropogenic processes and strongly related each other through a series of atmospheric chemical processes, the concurrent intra-species analyses can give valuable information about the relationships among pollutants and atmospheric processes. A first exploratory analysis of pollutant pairs was carried out by using bivariate level-plots, which substantially map the density of experimental data (i.e. the number of observations recorded for each couple of variables). Results are calculated overall the whole dataset (Fig. 5) and on a seasonal basis (Fig. SI4) and show prevailing levels of  $\text{NO}_2$  with respect to NO, which are more evident in the warm semester due to the potential fast oxidation of NO to  $\text{NO}_2$  by ozone and radicals. The inverse relationship of  $\text{NO}_2$  and ozone is less evident in the coldest season. No differences in the ratios of  $\text{NO}_2$  and  $\text{SO}_2$  between semesters have been evidenced. All BTEX appear to be correlated to each other in both semesters and their inverse relationship with OX levels is more evident in the warm period due to the highest OX concentrations.

A study on the relationships between the wind speed and pollutant concentrations was preliminarily carried out to investigate the effects and the frequency of the various conditions favouring the accumulation or the dispersion of pollutants in the atmosphere. The whole dataset

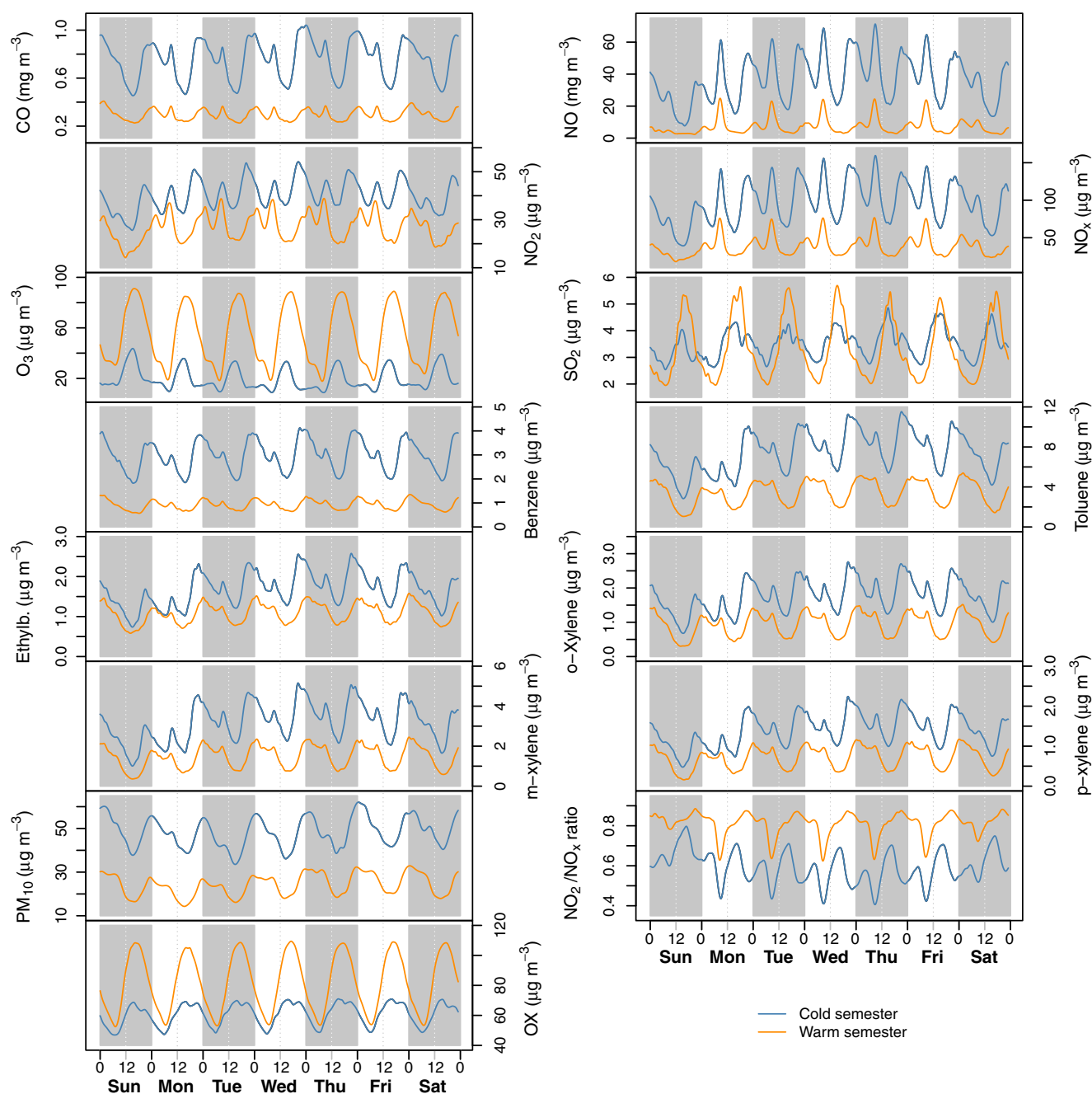


Fig. 4. Weekly and hourly-resolved average cycles calculated over the cold and warm semesters. Semesters were set accordingly to DST time in Italy.

was thus split into three groups, i.e. wind calm ( $\leq 0.5 \text{ m s}^{-1}$ ), moderate winds ( $>0.5$  and  $\leq 2.5 \text{ m s}^{-1}$ ) and strong winds ( $>2.5 \text{ m s}^{-1}$ ). The results are reported as Fig. S15 and show the inverse relationship between wind speed and the air pollutants mainly linked to traffic, i.e. CO, nitrogen oxides, BTEX and  $\text{PM}_{10}$ . On the contrary,  $\text{SO}_2$  and ozone increase when wind speed also increases, but this behaviour may be affected by the generally higher average wind speeds recorded in summer due to the occurrence of sea/land breezes.

A cross-correlation function (CCF at  $\pm 48 \text{ h}$  lag time) analysis was further performed to point out the relationships among the pollutants and between pollutants and weather parameters in more detail. CCFs have been computed separately for each season and most important relationships are reported in Fig. 6, while CCFs for additional pairs of variables are supplied as Fig. S16. Having similar daily cycles, most pollutants are characterized by highly positive or negative correlations

near the 0 h lag and, thus, at backward and forward 12 h intervals. As expected, ozone and solar irradiation show highly positive correlations during the whole year, increasing in summer and decreasing in winter at 24 h lags. However, a delay of the best correlations between ozone and solar radiation is also detected, meaning that the peak  $\text{O}_3$  concentrations are reached 1–3 h after the hours the solar light is the most intense. The effects of the photochemistry of the  $\text{NO}$ – $\text{NO}_2$ – $\text{O}_3$  system are highlighted by analyzing the  $\text{NO}$ – $\text{O}_3$  and  $\text{NO}_2$ – $\text{O}_3$  pairs, which show maximum negative correlations at lags 0,  $\pm 24 \text{ h}$  and  $\pm 48 \text{ h}$ . Despite the oxidation of NO by ozone and hydroxyl radical is recognized to be relatively fast (on a timescale of minutes, Finlayson Pitts and Pitts, 2000), a delay of about 1–2 h is generally observed for  $\text{NO}$ – $\text{O}_3$ , while no delay is evident for  $\text{NO}_2$ – $\text{O}_3$ . The CCF for  $\text{NO}$ – $\text{NO}_2$  clearly indicates increasing correlations at lags 0, 12, 24 h. Despite characterized by similar daily cycles, ozone and  $\text{SO}_2$  do not show highly positive correlations at 0



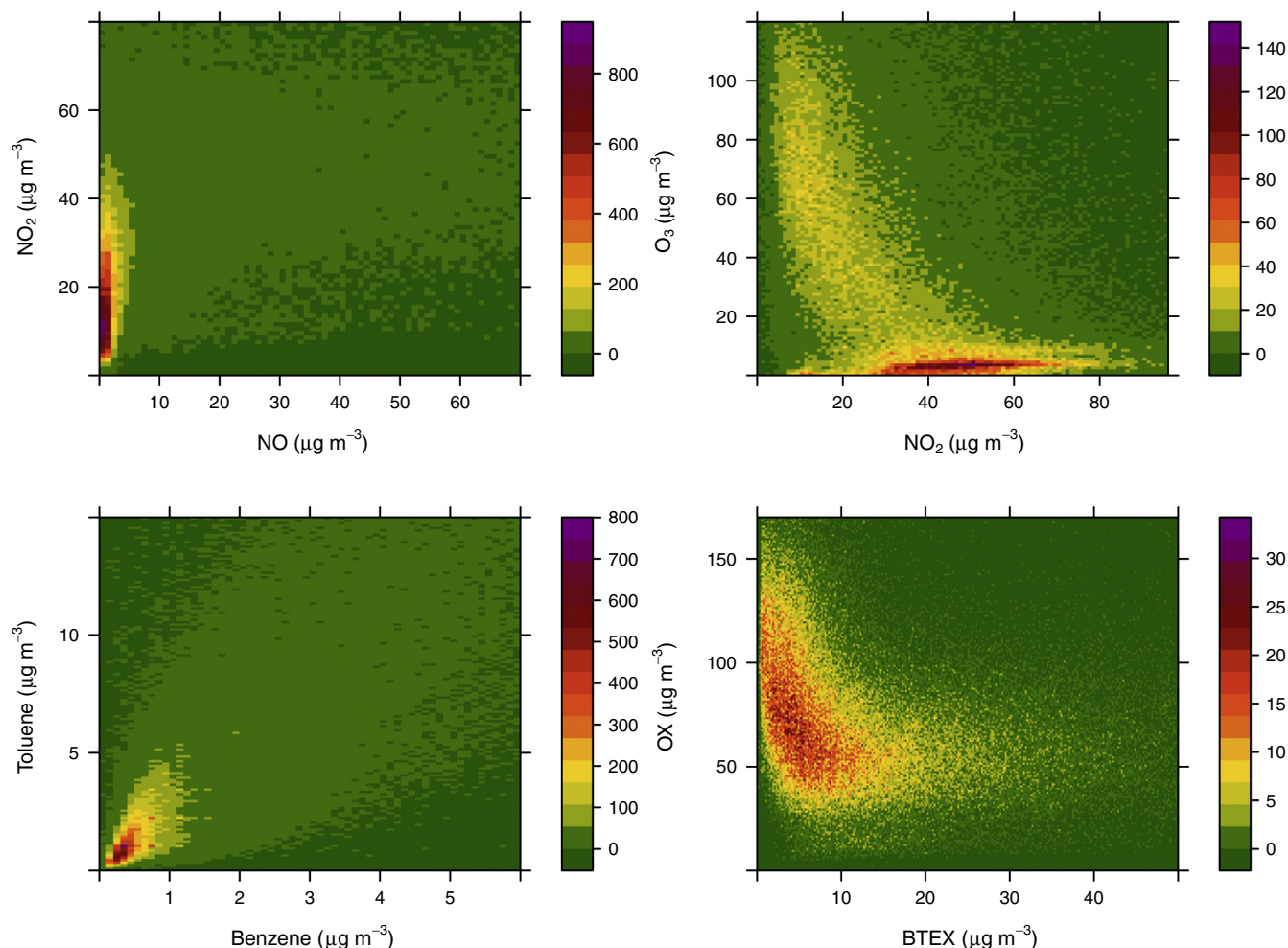


Fig. 5. Bivariate level-plots between pollutant pairs. The scale corresponds to the density of experimental data (i.e. the number of observations recorded for each couple of variables).

h lag, but exhibit negative correlations at 12 and 36 h lags. The role of oxidants in relation to oxidizable species (mainly CO and BTEX) is not straightforward, showing low negative ( $\sim 0.2$ ) correlations at 0 h and  $\pm 24$  h lags. Pairs between CO, NO, NO<sub>2</sub> and BTEX have highly positive correlations at 0 h lag, particularly due to the primary traffic emissions, and at 12 h interval lag backward and forward (i.e., 12, 24, 36 h) as well; while such pattern appears in all the seasons, correlations are generally higher in the coldest seasons. Similarly, PM<sub>10</sub> presents high correlations with CO, NO, NO<sub>2</sub> and BTEX, but with a 2–4 h delay, which may indicate a potential role of secondary processes on particulate matter nucleation and yield, i.e., the oxidation of nitrogen oxides to nitrate followed by the formation of ammonium nitrate and the oxidation of gaseous organics (BTEX in this case) to condensable semi-volatile species.

Fig. SI6 reports the lagged correlations between pollutant species and wind speed and gives some insights about the removal and accumulation processes: negative CCFs are commonly reported for WS and many species (CO, NO, NO<sub>2</sub>, BTEX, PM<sub>10</sub>) from 0 to 6 h lags, following the increased dilution through advection of external air masses and turbulence. On the contrary, ozone and SO<sub>2</sub> exhibit positive lagged correlations with WS: despite the SO<sub>2</sub>–WS correlations are observed only in summer and are low, the O<sub>3</sub>–WS correlations are high all over the year. This result is consistent with the hypothesis that external transport of air masses may have a strong influence on urban concentrations of ozone, as already reported in different coastal areas around the world during sea/land breeze events (e.g., Lin et al., 2007; Adame et al., 2010). The CCFs of pollutants with RH may be indicative of some atmospheric

processes; however RH has an evident diurnal pattern in the study area: higher values in early morning (0–8 am) and lower in early afternoon (1–4 pm), which is essentially driven by the diurnal pattern of the mixing height. Consequently, RH shows positive correlations with PM<sub>10</sub> and negative with SO<sub>2</sub> at 0 h lag. Despite atmospheric pressure has been used as an index of atmospheric stability, very low CCFs are recorded between pairs of pollutants and atmospheric pressure (Fig. SI6).

### 3.5. Relationships with the atmospheric circulation

Polar plots and CPF are reported in Fig. 7 and Fig. SI7, respectively. Polar plots were computed for each season, while CPF plots refer to the whole study period; wind calm ( $WS < 0.5 \text{ m s}^{-1}$ ) are excluded from the analysis. Generally polar plots of CO, NO<sub>x</sub>, and BTEX show increasing levels when air masses are close to the wind calm and slow winds from NW–WSW during the whole year, particularly in the coldest seasons (autumn and winter). This behaviour is also evidenced by CPF plots, which report higher (>90th percentile) concentrations when air masses blow from the 2nd quadrant, i.e. from a low-density residential area and the ring road, but not from the industrial area, city centre, airport and harbours. Similarly, CPF analysis reports higher concentrations of PM<sub>10</sub> from the 2nd quadrant, but polar plots clearly highlight increasing average concentrations when fast winds blow from the 1st and 4th quadrants, i.e. from the lagoon and the sea. This finding is more evident in winter. As evidenced by a recent source apportionment study (Masiol et al., 2012b), about 20% of PM<sub>10</sub> mass in winter is composed of sea-salt,

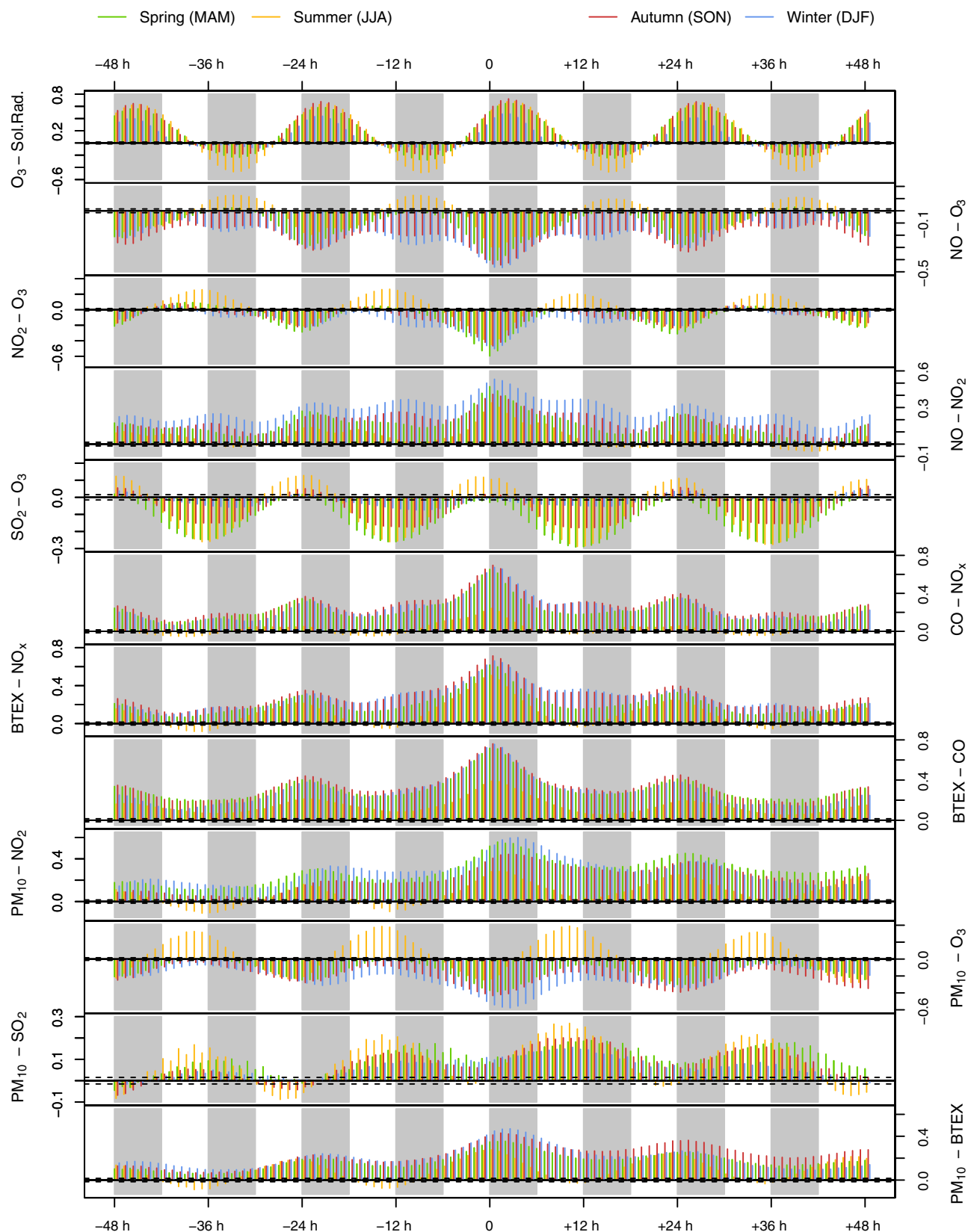


Fig. 6. Cross-correlations (at 48 h backward and forward) for hourly concentration of pairs of pollutants. Data are presented separately for each season.

which is mainly generated locally when moderately intense north-east winds pass over the coastline. Therefore, the results confirm the potential role of local sea-salt generation, playing a key role in enhancing  $PM_{10}$  concentrations in the study area.

Polar and CPF plots of ozone and  $SO_2$  have different behaviours. Ozone generally increases when air masses come from the 4th quadrant, while it drops when air masses move slowly. This result is consistent with the CCF analysis and points out the potential effect of external

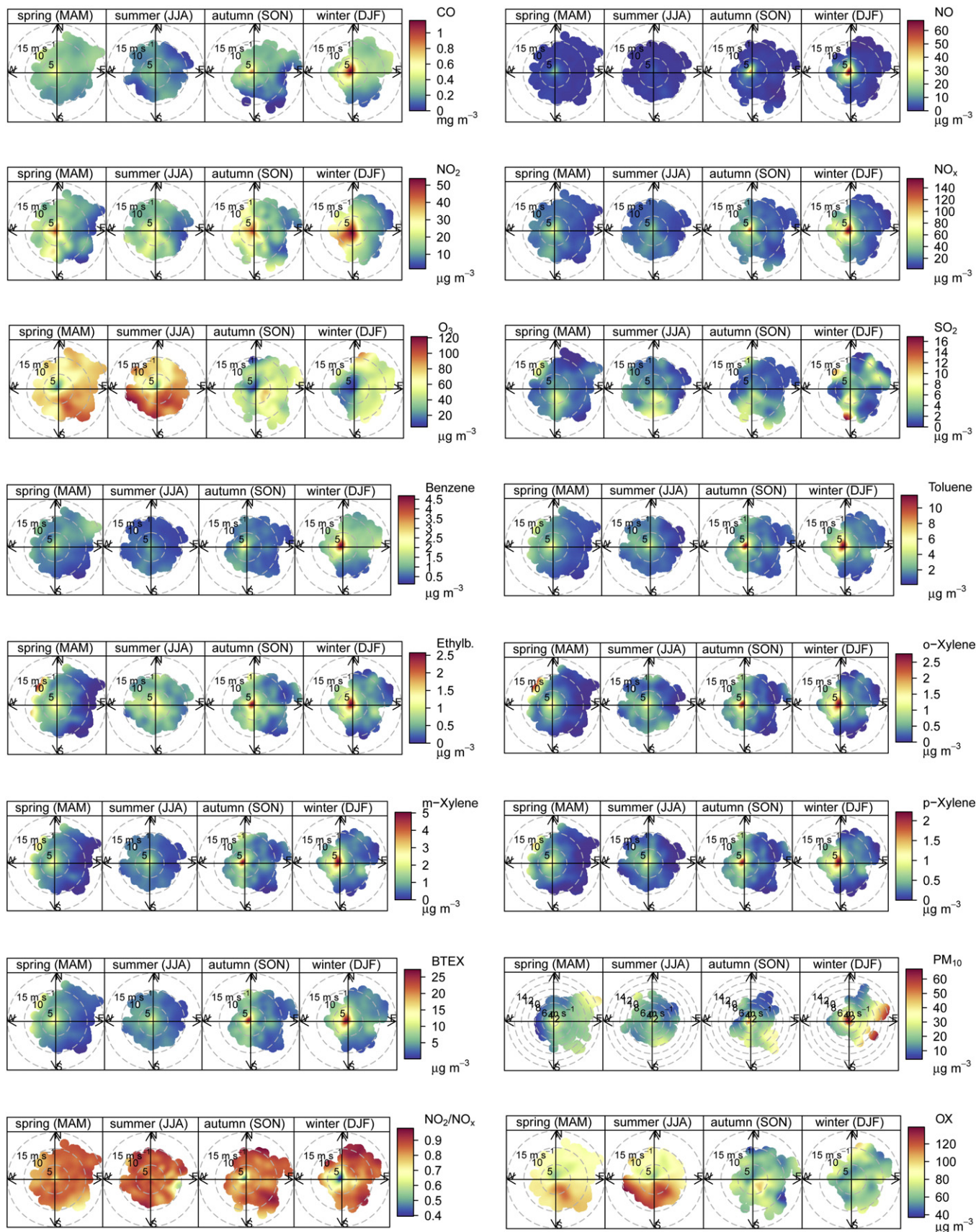


Fig. 7. Bivariate polar-plots of air pollutants calculated for each season of the study period.



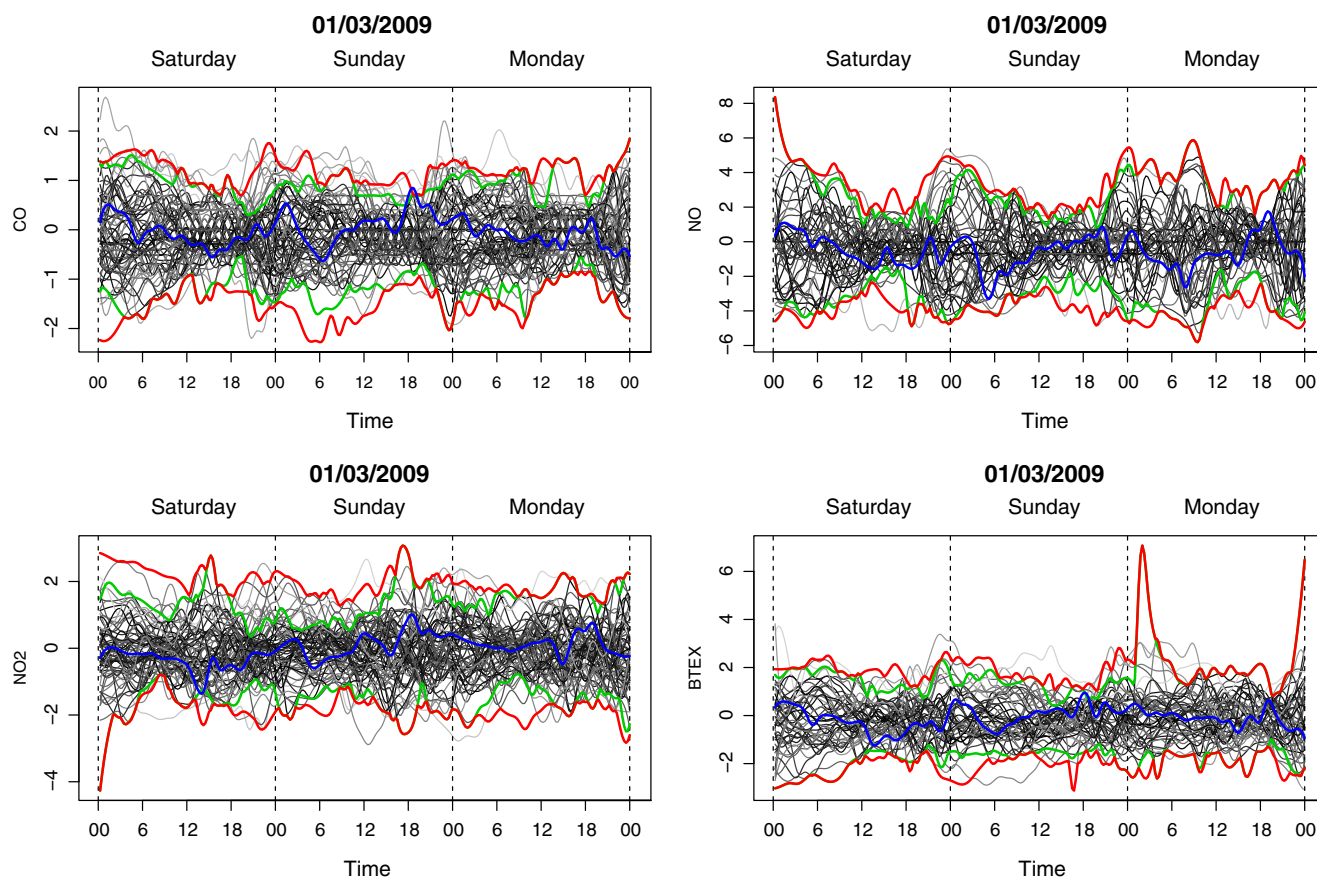


Fig. 8. Examples of log-ratios computed from the adopted statistical methodology.

transport of polluted air masses from the sea and surrounding rural environments. Both polar and CPF plots show that  $\text{SO}_2$  levels increase when air masses blow from south, i.e. from the industrial area and, thus, highlights the potential role of industrial emissions, which in the study area are dominated by coal power and oil refinery plants.

### 3.6. Effects of traffic-restricted Sundays upon air quality

Table 2 lists the traffic restricted Sundays imposed in the study area since November 2001. Some log-ratios computed from the adopted statistical methodology are shown in Fig. 8, while a comprehensive summary is provided in Figs. SI8–SI13. The 50th and 90th percentile confidence bands from modified half-region depth analysis are respectively green and red-coloured, TRS log-ratio series are in blue. In the vast majority of cases TRS series are within both boundary intervals, which somehow mark the variability (noise) of data, and it is not possible to determine any clear trend during the actions. On a statistical basis, results indicate that TRS have no significant impact on air quality. However, even if considering pollution data in periods supposed to be comparable, the data suffer from a large variability, which is mainly driven by weather rather than emissive factors. The variability inevitably increases the noise of data and boosts the confidence range, making the determination of statistically tangible effects more difficult. In addition, it should be remarked that TRS often diverts the traffic to the suburbs of Mestre, the ring road is never included in the actions and the surroundings towns are commonly not involved in traffic restrictions. It is therefore reasonable to state that the traffic is moved, rather than decreased. In conclusion, since TRS is unlikely to be prolonged over several consecutive days, it is evident that the traffic restrictions should be imposed simultaneously on a larger scale to produce real benefits, i.e. to the whole region or the whole Po Valley, rather than to few major cities only.

## 4. Conclusions

By providing direct information on the levels and trends of key pollutants, this study enables some general considerations to evaluate the air pollution extent and the effects of commonly adopted mitigation strategies in a large city of Po Valley, a remaining hotspot for air pollution in Europe. Some insights are provided to drive future successful plans and actions. The main results and conclusions can be summarized as follows:

- $\text{CO}$ ,  $\text{SO}_2$  and benzene levels were relatively low in the study period and EC thresholds, target and limit values were not exceeded. The  $\text{NO}_2$  annual average levels only exceeded the EC limit in 2003 (probably due to an extremely warm summer). On the contrary, ozone and  $\text{PM}_{10}$  were critical pollutants and alert thresholds and limit/objective values were frequently breached;
- emission inventories point out that the study area underwent a general drop of key pollutant emissions mainly due to the changes in the emissive scenarios. The analysis of long-term trends reveals a general good agreement for  $\text{CO}$ ,  $\text{SO}_2$  and benzene. While inventories assess an overall drop of  $\text{NO}_x$  emissions mainly due to decreasing power plant emissions and road traffic, STL reveals no significant variations over the study period and no changes in the  $\text{NO}_2/\text{NO}_x$  ratio. These results may suggest some further considerations: (i) despite the improvement of the road vehicle technology, the traffic volume has increased by making a null balance; (ii) the contribution of other sources may be more important; and (iii) the displacement of traffic from the ring road to an outside highway has not improved urban air quality;
- the seasonal, weekly and diurnal cycles of each pollutant were investigated and their shapes were discussed on the basis of emission factors, human habits, photochemical processes and weather. Typical sinusoidal seasonality and bimodal daily cycles are reported for most pollutants. Species mainly linked to road vehicle exhaust emissions ( $\text{CO}$ ,

- NO, NO<sub>2</sub>, BTEX) have a bimodal structure due to the peaks in traffic at 7–9 am and 6–8 pm, while ozone mainly follows the sunlight strength. The effect of night-time drop of the mixing layer height probably extends and amplifies the evening peak, while photochemical reactions and atmospheric circulation due to sea/land breezes may have an effect on the dilution of pollutants at midday;
- intra-species analysis was performed by means of cross-correlations. Highly positive lagged correlations are calculated at 0 h lag and, thus, at backward and forward 24 h intervals for all the pollutants from vehicular traffic (CO, NO, NO<sub>2</sub>, all BTEX) and between ozone and solar irradiance. A delay of about 1–2 h is generally observed for NO–O<sub>3</sub>, while a delay for NO<sub>2</sub>–O<sub>3</sub> is not evident;
  - generally, significant negative lagged correlations are reported between wind speed and CO, NO<sub>x</sub>, BTEX and PM<sub>10</sub>, but with a delay of 1–6 h;
  - polar plots and conditional probability function analysis were performed to locate the emission sources with respect to the sampling site. Results show that: (i) CO, NO<sub>x</sub>, and BTEX are mainly derived from residential areas and from the ring road; (ii) ozone increases when air masses come from the 4th quadrant due to the sea/land breezes and the potential influence of external transport is hypothesized; (iii) SO<sub>2</sub> is mainly due to the industrial emissions, as its levels increase when air masses blow from South and (iv) most probable sources of PM<sub>10</sub> are in the urban area, mainly due to traffic; however the potential role of sea-salt generation from the nearby lagoon and sea is also revealed;
  - a statistical approach is presented to analyze the effect of traffic-restricted Sundays upon air quality. Results generally show no significant changes or trends between TRS and non-TRS periods and enable some considerations about the potential benefit of such “short-term” measures to mitigate air pollution. TRS actions so far imposed at local level are demonstrated to have poor effects upon local air quality and such measures should be extended over a wider area.

## Disclaimer

This research was not funded by public or private institutions. The views expressed in this paper are exclusively of the authors and may not reflect those of ARPAV.

## Acknowledgments

This study is the document no. 3 of a cooperation between the Ca' Foscari University of Venice and ARPAV. A series of weather data were provided by Ente della Zona Industriale di Porto Marghera ([www.entezona.it](http://www.entezona.it)).

## Appendix A. Supplementary data

Supplementary data to this article can be found online at <http://dx.doi.org/10.1016/j.scitotenv.2014.06.122>.

## References

- Adame JA, Serrano E, Bolívar JP, De la Morena BA. On the tropospheric ozone variations in a coastal area of southwestern Europe under a mesoscale circulation. *J Appl Meteorol Climatol* 2010;49(4):748–59.
- ARPAV (Agenzia Regionale per la Prevenzione e Protezione Ambientale del Veneto). Monitoring of air pollutants; 2014 [Available at: <http://www.arpa.veneto.it/temi-ambientali/aria/emissioni-di-inquinanti/monitoraggio> (last accessed: January 2014)] [in Italian].
- Ashbaugh LL, Malm WC, Sadeh WZ. A residence time probability analysis of sulfur concentrations at Grand Canyon National Park. *Atmos Environ* 1985;19(8):1263–70.
- Atkinson R, Arey J. Atmospheric degradation of volatile organic compounds. *Chem Rev* 2003;103:4605–38.
- Baltaretu CO, Lichtman EI, Hadler AB, Elrod MJ. Primary atmospheric oxidation mechanism for toluene. *J Phys Chem A* 2009;113(1):221–30.
- Bigi A, Harrison RM. Analysis of the air pollution climate at a central urban background site. *Atmos Environ* 2010;44:2004–12.
- Bigi A, Ghermandi G, Harrison RM. Analysis of the air pollution climate at a background site in the Po valley. *J Environ Monit* 2012;14:552–63.
- Carlsaw DC. The openair manual – open-source tools for analysing air pollution data. Manual for version 0.8-0. London: King's College; 2013.
- Carlsaw DC, Ropkins K. openair – an R package for air quality data analysis. *Environ Model. Softw* 2012;27–28:52–61.
- Carlsaw DC, Beevers SD, Ropkins K, Bell MC. Detecting and quantifying aircraft and other on-airport contributions to ambient nitrogen oxides in the vicinity of a large international airport. *Atmos Environ* 2006;40(28):5424–34.
- Caselli M, de Gennaro G, Marzocca A, Trizio L, Tutino M. Assessment of the impact of the vehicular traffic on BTEX concentration in ring roads in urban areas of Bari (Italy). *Chemosphere* 2010;81(3):306–11.
- CAV (Concessioni Autostradali Venete). Financial statements at 31 December 2010; 2011 [In Italian].
- Cleveland RB, Cleveland WS, McRae JE, Terpenning I. STL: a seasonal-trend decomposition procedure based on loess. *J Off Stat* 1990;6(1):3–73.
- Curci G, Beekmann M, Vautard R, Smiatek G, Steinbrecher R, Theloke J, et al. Modelling study of the impact of isoprene and terpene biogenic emissions on European ozone levels. *Atmos Environ* 2009;43:1444–55.
- Cyrys J, Eeftens M, Heinrich J, Ampe C, Armengaud A, Beelen R, et al. Variation of NO<sub>2</sub> and NO<sub>x</sub> concentrations between and within 36 European study areas: results from the ESCAPE study. *Atmos Environ* 2012;62:374–90.
- EEA (European Environment Agency). AirBase—the European air quality database; 2014 [Available at: [www.eea.europa.eu/themes/air/air-quality/map/airbase](http://www.eea.europa.eu/themes/air/air-quality/map/airbase) (last accessed: January, 2014)].
- EZI (Ente della Zona Industriale di Porto Marghera). Report of the President to the assembly members; 2012 [In Italian].
- Fenger J. Air pollution in the last 50 years – from local to global. *Atmos Environ* 2009;43(1):13–22.
- Finlayson-Pitts BJ, Pitts JN. Chemistry of the upper and lower atmosphere: theory, experiments, and applications. San Diego: Academic Press; 2000.
- Grice S, Stedman J, Kent A, Hobson M, Norris J, Abbott J, et al. Recent trends and projections of primary NO<sub>2</sub> emissions in Europe. *Atmos Environ* 2009;43(13):2154–67.
- Hoor P, Borken-Kleefeld J, Caro D, Dessens O, Endresen O, Gauss M, et al. The impact of traffic emissions on atmospheric ozone and OH: results from QUANTIFY. *Atmos Chem Phys* 2009;9:3113–36.
- Hyslop NP. Impaired visibility: the air pollution people see. *Atmos Environ* 2009;43:182–95.
- ISPRA (Italian Institute for Environmental Protection and Research). Disaggregated national emission inventory 2010; 23014; 2014 [Available at: <http://www.sinanet.isprambiente.it/it/sia-ispra/inventaria/versione-2.0-dell2019inventario-provinciale-delle-emissioni-in-atmosfera/view> (last accessed: January 2014)].
- ISTAT (Italian National Institute of Statistics). Resident municipal population by age, sex and marital status metadata. Population on 1st January 2011; 2012 [Available at: <http://dati.istat.it/> (last accessed November, 2012)].
- Khoder MI. Ambient levels of volatile organic compounds in the atmosphere of Greater Cairo. *Atmos Environ* 2007;41:554–66.
- Kley D, Kleinmann M, Sanderman H, Krupa S. Photochemical oxidants: state of the science. *Environ Pollut* 1999;100:19–42.
- Laumbach RJ, Kipen HM. Respiratory health effects of air pollution: update on biomass smoke and traffic pollution. *J Allergy Clin Immunol* 2012;129(1):3–11.
- Lin C-H, Lai C-H, Wu Y-L, Lin P-H, Lai H-C. Impact of sea breeze air masses laden with ozone on inland surface ozone concentrations: a case study of the northern coast of Taiwan. *J Geophys Res* 2007;112:D14309. <http://dx.doi.org/10.1029/2006JD008123>.
- Lopez-Pintado S, Romo J. A half-region depth for functional data. *Comput Stat Data Anal* 2011;55(4):1679–95.
- Masiol M, Hofer A, Squizzato S, Piazza R, Rampazzo G, Pavoni B. Carcinogenic and mutagenic risk associated to airborne particle-phase polycyclic aromatic hydrocarbons: a source apportionment. *Atmos Environ* 2012a;60:375–82.
- Masiol M, Squizzato S, Ceccato D, Rampazzo G, Pavoni B. Determining the influence of different atmospheric circulation patterns on PM10 chemical composition in a source apportionment study. *Atmos Environ* 2012b;63:117–24.
- Maynard RL. Health effects of urban pollution. In: Hester RE, Harrison RM, editors. *Issues in environmental science and technology* no. 28. Cambridge: Royal Society of Chemistry; 2009. p. 108–28.
- R Core Team. R: a language and environment for statistical computing. Vienna, Austria: R Foundation for Statistical Computing; 2013 [Available at: <http://www.R-project.org/>].
- SAVE. Statistics and traffic of Venice Airport system webpage; 2012 [Available at: <http://www.veniceairport.it> (last accessed December, 2012)].
- Seinfeld JH, Pandis SN. Atmospheric chemistry and physics – from air pollution to climate change. 2nd ed. New York: John Wiley & Sons; 2006.
- Sen PK. Estimates of the regression coefficient based on Kendall's tau. *Journal of the American Statistical Association* 1968;63:1379–89.
- Solberg S, Hov Ø, Søvde A, Isaksen ISA, Coddeville P, De Backer H, et al. European surface ozone in the extreme summer 2003. *J Geophys Res* 2008;113(D7). <http://dx.doi.org/10.1029/2007JD009098>.
- Squizzato S, Masiol M, Brunelli A, Pistollato S, Tarabotti E, Rampazzo G, et al. Factors determining the formation of secondary inorganic aerosol: a case study in the Po Valley (Italy). *Atmos Chem Phys* 2013;13:1927–39.
- Theil H. A rank-invariant method of linear and polynomial regression analysis. In: Henri Theil's Contributions to Economics and Econometrics. Springer Netherlands; 1992. p. 345–81.
- Vardoulakis S, Gonzales-Flesca N, Fisher BEA. Assessment of traffic-related air pollution in two street canyons in Paris: implications for exposure studies. *Atmos Environ* 2002;36:1025–39.
- Venice Port Authority (Autorità Portuale di Venezia). Relazione annuale 2009; 2010 [in Italian].
- Watt J, Tidblad J, Kucera V, Hamilton R. The effects of air pollution on cultural heritage. New York: Springer; 2009.
- WHO (World Health Organization). Air quality guidelines for Europe. 2nd ed. Copenhagen: WHO, Regional Office for Europe; 2000.